

Published in final edited form as:

Neurobiol Dis. 2011 October ; 44(1): 63–72. doi:10.1016/j.nbd.2011.06.004.

Low dose dextromethorphan attenuates moderate experimental autoimmune encephalomyelitis by inhibiting NOX2 and reducing peripheral immune cells infiltration in the spinal cord

Olga V. Chechneva^a, Florian Mayrhofer^a, Daniel J. Daugherty^a, David E. Pleasure^b, Jau-Shyong Hong^c, and Wenbin Deng^{a,b}

^a Department of Cell Biology and Human Anatomy, School of Medicine, University of California-Davis, 2425 Stockton Blvd, Sacramento, 95817 CA

^b Institute for Pediatric Regenerative Medicine, Shriners Hospitals for Children, 2425 Stockton Blvd, Sacramento, 95817 CA

^c Neuropharmacology Section, Laboratory of Pharmacology and Chemistry, National Institute of Environmental Health Sciences, Research Triangle Park, 27709 NC

Abstract

Dextromethorphan (DM) is a dextrorotary morphinan and a widely used component of cough medicine. Relatively high doses of DM in combination with quinidine are used for the treatment of mood disorders for patients with multiple sclerosis (MS). However, at lower doses, morphinans exert anti-inflammatory activities through the inhibition of NOX2-dependent superoxide production in activated microglia. Here we investigated the effects of high (10 mg/kg, i.p., “DM-10”) and low (0.1 mg/kg, i.p., “DM-0.1”) doses of DM on the development and progression of mouse experimental autoimmune encephalomyelitis (EAE), an animal model of MS. We found no protection by high dose DM treatment. Interestingly, a minor late attenuation by low dose DM treatment was seen in severe EAE that was characterized by a chronic disease course and a massive spinal cord infiltration of CD45⁺ cells including T-lymphocytes, macrophages and neutrophils. Furthermore, in a less severe form of EAE, where lower levels of CD4⁺ and CD8⁺ T-cells, Iba1⁺ microglia/macrophages and no significant infiltration of neutrophils were seen in the spinal cord, the treatment with DM-0.1 was remarkably more beneficial. The effect was the most significant at the peak of disease and was associated with an inhibition of NOX2 expression and a decrease in infiltration of monocytes and lymphocytes into the spinal cord. In addition, chronic treatment with low dose DM resulted in decreased demyelination and reduced axonal loss in the lumbar spinal cord. Our study is the first report to show that low dose DM is effective in treating EAE of moderate severity. Our findings reveal that low dose morphinan DM treatment may represent a new promising protective strategy for treating MS.

© 2011 Elsevier Inc. All rights reserved.

Corresponding author: Wenbin Deng, UC Davis School of Medicine, 2425 Stockton Boulevard, Room 653B, Sacramento, CA, 95817, Fax: (916) 453-2288, Phone: (916) 453-2287, wbdeng@ucdavis.edu.

Publisher's Disclaimer: This is a PDF file of an unedited manuscript that has been accepted for publication. As a service to our customers we are providing this early version of the manuscript. The manuscript will undergo copyediting, typesetting, and review of the resulting proof before it is published in its final citable form. Please note that during the production process errors may be discovered which could affect the content, and all legal disclaimers that apply to the journal pertain.

Keywords

Low dose dextromethorphan; EAE; NOX2 NADPH oxidase; microglia; CNS infiltration; demyelination; axonal loss

Introduction

Multiple sclerosis (MS) is an autoimmune demyelinating disease characterized by chronic inflammation and axonal loss in the central nervous system (CNS). Treatment of MS is limited to immunomodulatory or immunosuppressive therapy that is not always successful and often has severe adverse effects (Gold et al., 2006). Therefore, the search for new compounds that can regulate autoimmune inflammation without causing significant side effects is of importance. Derivatives of morphine have been reported to attenuate inflammation in chronic neurodegenerative disorders (Li et al., 2005; Liu and Hong, 2003; Zhang et al., 2004). This anti-inflammatory effect was observed with both dextra- and levorotary morphinans, was not associated with opioid receptor modulation, and was due to the inhibition of superoxide production by phagocytic nicotinamide adenine dinucleotide phosphate (NADPH) oxidase NOX2 (Li et al., 2005; Liu et al., 2000; Liu et al., 2003; Qin et al., 2005). Anecdotally, an antagonist of opioid receptors, naltrexone, has been prescribed off-label at low doses for the treatment of several autoimmune disorders, including MS. The effect of “low dose naltrexone” (LDN) is believed to be mediated through the increase of opioid receptors density induced by chronic application of opioid antagonists (Narita et al., 2001; Rajashekara et al., 2003). It is unclear whether inhibition of NOX2 might also contribute in the protective effect of LDN.

NOX2 is highly expressed in phagocytic cells including macrophages, neutrophils and microglia. Activation of NOX2 requires the assembly of an enzyme complex consisting of the cytosolic subunits p47phox, p40phox, p67phox and a membrane bound flavocytochrome gp91phox (NOX2) associated with p22phox (Bedard and Krause, 2007). Superoxide produced by NOX2 is involved in a cascade of reactions generating other reactive oxygen species (ROS) (Lam et al., 2010). The role of ROS in autoimmune diseases remains unclear. It has been shown that p47phox knockout mice are resistant to experimental autoimmune encephalomyelitis (EAE) (van der Veen et al., 2000). Mice carrying a mutation in the p47phox encoding gene *Ncf1* showed amelioration of EAE symptoms when EAE was induced with a myelin oligodendrocyte glycoprotein (MOG) peptide. However, using the entire MOG protein resulted in an exacerbation of EAE in *Ncf1* mutated mice, suggesting a regulatory role of ROS in the function of antigen-presenting cells (Hultqvist et al., 2004). In addition, NOX2^{-/-} dendritic cells showed a drastic decrease in antigen cross presentation and initiation of adaptive immunity (Savina et al., 2006). NOX2 derived ROS produced by perivascular macrophages and endothelial cells increased the permeability of the blood brain barrier that contributes to the subsequent trafficking of pathogenic mononuclear cells into the CNS (Huppert et al., 2010; Mirshafiey and Mohsenzadegan, 2009). Chemotaxis of phagocytic cells to the site of inflammation is also regulated by ROS (Hattori et al., 2010). Indeed, microglia play a substantial role in the development of autoimmune CNS inflammation. Resident microglia are activated preferentially by Th17 or Th1/Th17 T-lymphocytes invading the CNS before the development of clinical symptoms of EAE (Murphy et al., 2010). Microglial activation is associated with an upregulated expression of MHC class II, release of pro-inflammatory cytokines, chemokines and ROS that attract peripheral immune cells and cause damage to oligodendrocytes and neurons (Benveniste, 1997; Gandhi et al., 2010; Szczucinski and Losy, 2007).

Dextromethorphan (DM) is a morphinan widely used as a component of cough medicine. DM is a weak inhibitor of serotonin reuptake and in combination with quinidine, which prevents O-demethylation of DM, is promoted by Avanir Pharmaceuticals Inc. for the treatment of pseudobulbar affect in patients with MS and amyotrophic lateral sclerosis. Lacking the affinity to opioid receptors, DM works as a non-competitive antagonist of NMDA receptors, inhibits voltage gated Ca^{2+} -channels, and stimulates sigma-1 receptors at relatively high doses (Werling et al., 2007). Due to these properties, DM has been shown to be neuroprotective in models of cerebral ischemia, spinal cord injury, epilepsy and Parkinson's disease (Britton et al., 1997; Kim et al., 1996; Steinberg et al., 1988; Topsakal et al., 2002; Zhang et al., 2004). At lower doses, DM or other morphinans are known to inhibit NOX2 mediated production of ROS in activated microglia/macrophages by the reduction of p47phox translocation to the cell membrane through the inhibition of ERK 1/2 phosphorylation (Liu et al., 2009; Qian et al., 2007).

Here we studied the effects of high-dose versus low-dose DM treatment on the development and progression of mouse EAE, an animal model of MS. We also investigated possible mechanisms of action.

Material and Methods

Animals

Experiments were carried out in accordance with the National Institutes of Health guidelines for the use of laboratory animals; all animal protocols were approved by the University of California Davis Institutional Animal Care and Use Committee. A total of 56 C57BL/6 male mice (25–35 g) were obtained from Jackson Laboratories (Sacramento, CA). All efforts were made to minimize the numbers of animals used and to ensure minimal suffering.

Induction of EAE and DM treatment protocol

To induce EAE, C57/BL6 male mice of 8–12 weeks old were injected subcutaneously in the flank with an emulsion of MOG_{35–55} peptide in incomplete Freund's adjuvant supplemented with Mycobacterium tuberculosis H37Ra (M.t.). Using different concentrations of MOG/M.t., two types of EAE trials were initiated. *EAE-I* was induced with 300 μg of MOG and 2.5 mg/ml M.t., and *EAE-II* with 50 μg MOG and 0.5 mg/ml M.t. (Fig. 1A). Mice also received two i.p. injections of 250 ng of pertussis toxin immediately after immunization and 48 h later. Body weight and clinical signs of EAE were monitored daily. The severity of clinical symptoms was scored based on a standard neurological scoring system for EAE as follows: 0 – no deficit; 1 – complete loss of tail tone; 1.5 – mildly impaired righting reflex; 2 – abnormal gait (ataxia) and/or impaired righting reflex; 2.5 – single limb paresis and ataxia; 3 – double limb paresis; 3.5 – single limb paralysis and paresis of second limb; 4 – full paralysis of two limbs; 4.5 – moribund; 5 – dead (Selvaraj et al., 2009). Scoring was performed in a blind fashion. Beginning from day 7 post immunization (d.p.i.), animals received an i.p. injection of saline, DM 0.1 mg/kg (DM-0.1) or DM 10 mg/kg (DM-10) (Sigma) once daily. Based on the data of clinical score, each EAE was characterized using the following parameters: the number of days to onset, mean score at the peak of the disease, maximal severity score, duration of paralysis, mean score at the end of the experiment, and animal survival. Animals were monitored for 45 days and spinal cord tissue was collected for analysis at the end of each experiment. When necessary, tissue was also collected at the peak of disease for analysis.

RNA Isolation and qPCR

To examine the cellular compositions of spinal cord infiltrates and the relative expression of immune cytokines and NOX2 subunits, we performed real-time quantitative reverse

transcriptase-polymerase chain reaction (qPCR) analysis. Mice were anesthetized with ketamine:xylazine (100:10 mg/kg) and perfused through the heart with a phosphate-buffered saline (PBS). Lumbar spinal cords were carefully excised and stored separately in liquid nitrogen. Total RNA was isolated from spinal cord tissue using RNeasy Lipid Tissue Mini Kit (Qiagen) following the standard protocol. For quality control, RNA purity was verified using the OD260/280 ratio to be between 1.8 and 2.0. Total RNA (1 µg) was reverse-transcribed to cDNA using Multiscribe™ reverse transcriptase (Applied Biosystems). Subsequent qPCR reactions for GAPDH, CD45, CD11b, CD11c, Ly6g, gp91phox and p47phox were performed in triplicates on a Roche Lightcycler 480 using SYBR Green Master Mix (Roche Applied Science). Specific primers were designed using the Primer3 Input software. The following primers were used: GAPDH, forward: 5'-GCCTTCCGTGTTCTACC-3', reverse: 5'-GCCTGCTTCACCACCTTC-3'; CD45, forward: 5'-GAAGATGTGGTTGATGTT-3', reverse: 5'-GAACTGGTATTGCTCATAG-3'; CD11b, forward: 5'-TCAGAAGATGAAGGAGTT-3', reverse: 5'-CATTGAAGGTGAAGTGAA-3'; CD11c, forward: 5'-TTAACTTCTCAACCTCAG-3', reverse: 5'-TCTATTCCGATAGCATTG-3'; Ly6g, forward: 5'-GGAGATAGAAGTTATTGTG-3', reverse: 5'-CAGTATTGTCCAGAGTAG-3'; gp91phox, forward: 5'-CAGGAGTTCCAAGATGCCTG-3', reverse: 5'-GATTGGCCTGAGATTCATCC-3'; p47phox, forward: 5'-AGATCTCCCGCTGCCACAC-3', reverse: 5'-GCCCGATAGGTCTGAAGGATGATG-3'. The specificity of products from each primer set was validated by analyzing all melting curves (T_m). To examine the transcription levels of CD4, CD8, IFN- γ , iNOS and sigma-1 receptors, qPCR reactions were performed in duplicates using validated TaqMan gene expression assay (Applied Biosystems), CD4 (Mm00442754_m1), CD8 (Mm01182107_g1), INF- γ (Mm01168134_m1), IL-17 (Mm00439619_m1), iNOS (Mm00440502_m1), sigma-1 receptors (Mm00448086_m1). For both SYBR Green and TaqMan primers, validation was performed by calculating qPCR efficiencies by the amplification of a standardized dilution series, and constructing a relative efficiency plot comparing target and reference ΔC_p values to ensure that the absolute slope of fit line was less than 0.1. Subsequently, all experimental samples were analyzed and normalized with the expression level of the internal control gene, GAPDH. Relative quantification of fold-change was performed by applying the $2^{-\Delta\Delta C_t}$ method and comparing C_p values (calculated by second derivative maximum) of individual mice to CFA control mice (Livak and Schmittgen, 2001).

Histology and Immunohistochemistry

Mice were anesthetized, and lumbar spinal cords were dissected from transcardial perfusion-fixed animals and placed in 4% paraformaldehyde (PFA) for 24 h. Samples were then exposed to stepwise cryoprotectant equilibration in 10% and 20% sucrose and thereafter embedded in 20% sucrose/OCT (1:1; Sakura Finetek, Torrance, CA) and frozen in dry ice-cooled isopentane. The 14-µm thick sections were prepared in a cryotome and stored in PBS at 4°C until use.

For examination of myelin loss, sections were collected on glass slide and stained with Luxol Fast Blue (LFB). In brief, sections were washed with ddH₂O for 2 min and then placed in 70% and further 95% ethanol for 1 min. Samples were incubated in 0.1% LFB solution at 60°C for 16 h. After washing in 95% ethanol to remove excess stain, sections were incubated in 0.05% lithium carbonate. Slides were mounted using xylene-based Cytoseal XYL medium. Images were acquired on an Olympus BX61-DSU microscope (Olympus Corp., Melville, NY) using a Hamamatsu ORCA-ER camera (Hamamatsu Photonics, Shizuoka, Japan).

For immunostaining of myelin basic protein (MBP), Iba1, CD4, CD45 or SMI-312, sections were post-fixed in 4% PFA for 30 min. Endogenous peroxidase was inhibited by treatment with 1% H₂O₂ for 5 min. An antigen retrieval step using 10 mM sodium citrate was required for sections stained with SMI-32. Nonspecific binding of antibodies was blocked using 10% normal goat serum in 0.1% Triton X in PBS, and samples were then incubated with rat anti-MBP (1:100; Novus Biologicals, Littleton, CO), rabbit anti-Iba1 (1:500; Wako Chemicals Industries Ltd., Richmond, VA), rat anti-CD4 (BD Biosciences, San Jose, CA), rat anti-CD45 (1:200; SouthernBiotech, Birmingham, AL) or mouse anti-SMI-312 (1:500; Covance, Princeton, NJ) overnight at 4 °C. Slides were then washed in PBS and incubated with fluorophore-conjugated secondary antibody Alexa Fluor 488 or 555 (1:1000). Fluorescent nuclear counterstaining was carried out using 4,6-diamidino-2-phenylindole (1 μM final concentration; Invitrogen) for 10 min. Slides were then washed in PBS and mounted using ProLong Gold mounting medium (Invitrogen). Images were acquired on a Nikon Eclipse TE 2000-E microscope using a D-Eclipse C1si camera (Nikon Instruments Inc., Melville, NY). MBP-SMI⁺ and SMI⁺ axons were quantified in the blind fashion in the area 0.01 mm² located in white matter of the ventrolateral lumbar spinal cord.

Microglial cultures

Primary microglial cultures were prepared from P1-3 C57/Bl6 mice. In brief, cerebral cortices were isolated after the removal of meninges, homogenized with a fire-polished Pasteur pipette, and sequentially passed through an 18G, 22G and 25G needle syringe and a 40 μm cell strainer to collect dissociated cells in a 50 ml falcon tube. Cells were then washed with PBS, centrifuged for 10 min at 1000 rpm, incubated in DNase-I for 10 min at 37°C, again washed with PBS and centrifuged for another 5 min at 1200 rpm. After centrifugation cells were resuspended in DMEM/F12 (Gibco) supplemented with 2 mM L-glutamine, 10% endotoxin-free fetal bovine serum (HyClone) and 1% penicillin/streptomycin. Cells were plated on poly-D-lysine (PDL) coated 75-cm² flasks at a density of 5 × 10⁶ cells and maintained in a 37°C and 5% CO₂ incubator. The medium was changed the next day and once per week thereafter. After 10–14 days in vitro, microglia were harvested by shaking at 200 rpm for 1 h. Floating cells were collected and plated at a density of 5 × 10⁵ cells/well in PDL coated 24-well plates. The purity of the replated microglial cultures was 96% judged by FACS analysis of CD11b expression. In the next day, cells were washed with PBS and pretreated with different concentrations of DM (10⁻⁵ – 10⁻¹⁰ M) for 2 h at 37°C. INF-γ (20 ng/ml, Akron Biotechnology, Boca Raton, FL) was then added to the cultures, and cells were maintained for another 22 h at 37°C and then collected for further RNA isolation using RNeasy Mini Kit (Qiagen).

Superoxide production in microglia and spinal cord tissue

Superoxide production was measured by lucigenin-enhanced chemiluminescence in microglial cultures. N9 microglia were plated in a density of 2 × 10⁴ cells/well on a 96 well Optiplate (Perkin Elmer) and kept for 24 h at 37°C to attach. In the following day, cells were washed twice with Krebs-HEPES buffer and pretreated for 2 h with DM (10⁻⁵ – 10⁻¹⁵ M) or NADPH oxidase inhibitors diphenyliodonium chloride (DPI, 10 μM) or apocynin (1 mM) in Krebs-HEPES buffer. After stimulation with IFN-γ (20 ng/mL) for 10 min, cells were incubated with 5 μM lucigenin for 15 min at room temperature and NADPH (100 μM) was then added to the wells immediately before reading.

To measure superoxide production in the spinal cord, total proteins were isolated by homogenizing the tissue in Krebs-HEPES lysis buffer containing 1 mM EGTA, 1 mM EDTA, 0.1% Triton-X and protease and phosphatase inhibitors (Roche). Protein samples (150 μg/well) were prepared in a 96 well Optiplate and incubated with 5 μM lucigenin for 15 min at room temperature. NADPH was added to the wells immediately before reading.

Measurements were obtained for a total period 13 min. The luminescence in each well was detected 5 times during 2 seconds using Microbeta TriLux 1450 LSC & Luminescence Counter (Perkin Elmer, Waltham, MA). Numbers of all readings were summed and represented as relative luminescence units (RLU) or percentage to CFA group readings. Each of the reading samples was prepared in triplicates and each experiment was repeated twice.

Statistical analysis

All statistical analyses were performed using GraphPad Prism 5.0 (GraphPad Software Inc., San Diego CA). The statistical significance of differences between means was evaluated using one-way ANOVA followed by *post hoc* Newman–Keuls test for multiple comparisons or two-way ANOVA followed by Bonferroni posttest. Single comparisons were analyzed by the Student's t-test. For data not satisfying assumptions of normality and homogeneity of variance, a nonparametric Mann-Whitney test was used. In all figures, data are represented as mean \pm S.E.M. In all cases probability values less than 0.05 were considered statistically significant.

Results

Effect of DM on the development and progression of EAE

At doses ranging from 10–80 mg/kg, DM is neuroprotective in models of cerebral ischemia, spinal cord injury and epilepsy (Werling et al., 2007) due to the blockade of NMDA receptors and the stimulation of sigma-1 receptors (Kim et al., 2003). At lower doses, DM inhibits NOX2 activity and therefore has an anti-inflammatory effect. To study the effect of DM treatment on the development and progression of EAE, two dosing paradigms of DM, high dose DM-10 and low dose DM-0.1, were used.

To account for EAE developments involving different pathological mechanisms and phenotypes in the same strain of animals (Berard et al., 2010), we performed EAE trials using different concentrations of MOG/M. t. (Fig. 1A). *EAE-I*: 300 μ g MOG and 2.5 mg/ml M.t.; *EAE-II*: 50 μ g MOG and 0.5 mg/ml M.t. Animals were treated daily with DM-10, DM-0.1 or saline starting from day 7 after EAE induction (Fig. 1B). In *EAE-I*, all animals developed paralysis with the peak at day 16–19 after EAE induction and the average maximal severity score of EAE was 4.2 ± 0.1 (Fig. 1C; Table 1). Neither DM-10 nor DM-0.1 treatment could ameliorate the onset or progression of the disease (Table 1). Although DM was not effective against this form of severe EAE, we still could observe a minor late neuroprotective effect of DM-0.1 around 30 d.p.i. To stimulate the relapsing–remitting form of MS (RRMS) with less severe EAE, we followed the protocol suggested previously by Berard et al. (2010). Although a decrease of MOG and M.t. did not result in a definitive RRMS pattern in *EAE-II*, under these conditions, DM-0.1 could significantly attenuate the development of the peak of the disease (Table 2; mean clinical score 2.2 ± 0.5 in DM-0.1 versus 3.6 ± 0.2 in saline) and slightly reduced EAE progression (Fig. 1D). The maximal severity score in DM-0.1 treated group was 3.7 ± 0.2 in comparison to 4.1 ± 0.1 in the saline group (Table 2). A non-significant remission of clinical symptoms was observed after the EAE peak in DM-10 treated group in *EAE-II*, but neither low dose DM-0.1 nor high dose DM-10 could change the onset or duration of paralysis compared to saline (Table 2). Thus, the effect of DM treatment in EAE was dependent on the induction of EAE and the development of the disease. A reduction of MOG and M.t. resulted in a moderate EAE that revealed a beneficial effect of DM-0.1. No protection was observed with DM-10.

The moderate EAE displays a lower level of immune cell infiltration into the spinal cord

Next, we compared the pathology of *EAE-I* and *EAE-II* in order to define the factors that may be important for the neuroprotective effect of DM. To reveal the differences between *EAE-I* and *EAE-II*, the pathological phenotypes, the severity of demyelination and the pattern of CNS infiltration were compared using the clinical scores and histology of the spinal cords tissue of saline treated animals. While *EAE-I* showed a 100% incidence of the disease (Table 1), a decrease in MOG/M.t. in *EAE-II* resulted in the reduction of the incidence to 96% (Table 2). There were no significant differences in the time of onset, the clinical score at the peak of disease or the maximal severity score between *EAE-I* and *EAE-II*. An increase of the survival rate was found in *EAE-II* compared to *EAE-I*. None of the EAE trials showed a particularly significant remission of clinical symptoms during the observation period (45 days), similar to the chronic-progressive form of EAE described previously (Berard et al., 2010). Histological analysis of the spinal cords was performed at the peak (19–20 d.p.i.) and in the chronic phase of EAE (45 d.p.i.). At both time points we found CD4⁺ T-lymphocytes localized in the spinal cord parenchyma of *EAE-I* (Fig. 2B, 2D) and *EAE-II* animals (Fig. 2C, 2E). The numbers of CD4⁺ cells were significantly elevated at the peak of *EAE-I* (Fig. 2B) and *EAE-II* (Fig. 2C) when compared to the CFA-control group (Fig. 2A) where no cells expressing CD4 antigen were observed. In addition, a significant upregulation of CD4 (Fig. 2L) and CD8 (Fig. 2M) mRNA was detected at the peak of *EAE-I* and *EAE-II* in comparison to CFA-control. A high amount of T-cells was still seen in the spinal cord parenchyma in *EAE-I* during the chronic phase of disease (Fig. 2D, 2L, 2M) whereas *EAE-II* showed a minor level of T-cell infiltration at this time point (Fig. 2E, 2L, 2M). We found an intact myelin layer, evenly stained with LFB in coronal sections of the CFA-only control animals (Fig. 2F). Demyelinating plaques and areas with damaged myelin were mostly seen in the ventrolateral part of the spinal cords of *EAE-I* (Fig. 2G) and *EAE-II* (Fig. 2H) animals. However, in *EAE-I* demyelination was profoundly progressed. A dramatic upregulation of the transcript of the microglia/macrophages marker CD11b was found at the peak of *EAE-I* by qPCR (Fig. 2N). In *EAE-II*, this increase was less prominent but still significant in comparison to CFA-control. At the later time point the level of CD11b mRNA was reduced in both EAEs (Fig. 2N), however in *EAE-I* it was still elevated when compared to CFA-control or *EAE-I*. This observation was confirmed by immunohistochemistry for the microglia/macrophage marker Iba1 (Fig. 2I, 2J, 2K). Iba1⁺ cells were accumulated prominently on the site of demyelination. A high amount of CD45⁺ cells was also monitored in the spinal cords of *EAE-I* animals during the chronic phase of disease (Fig. 2J, 2K). The majority of round Iba1⁺ cells found in *EAE-I* expressed CD45 and was identified as activated macrophages, whereas Iba1⁺ cells with weak CD45 expression were considered to be microglia. Interestingly, a significant increase of neutrophils expressing Ly6g mRNA was found only at the peak of *EAE-I* and some Ly6g expression was also detected at the chronic phase (Fig. 2O). In *EAE-II* no significant level of Ly6g was observed at the peak, but a small increase was found at the later stage. Although the mRNA level of dendritic cell marker CD11c was elevated in EAE mice compared to the CFA control, there were no differences detected in CD11c gene expression between *EAE-I* and *EAE-II*. Thus, we found that *EAE-I* was characterized by a chronic pattern of clinical phenotype, high severity, an increased infiltration of macrophages, T-lymphocytes and neutrophils into the spinal cord and an upregulation of microglia. Spinal cord infiltration in *EAE-I* was more severe compared to *EAE-II* that displayed an alleviated form of EAE characterized by a chronic type of disease with moderate severity and periods of slight remission and with lower CNS infiltration.

DM-0.1 treatment prevents infiltration of peripheral immune cells into the CNS in moderate EAE

Since the beneficial effect of low dose DM treatment was the most prominent at the peak of *EAE-II*, we next investigated whether the DM treatment could affect the infiltration of peripheral immune cells into the CNS. Spinal cord tissue of *EAE-II* animals was collected at the peak of EAE and examined for the transcription levels of mRNAs encoding proteins characteristic of peripheral immune cells. Lower levels of CD45 (Fig. 3A) and CD11b mRNA (Fig. 3B) were found in the DM-0.1 treated group ($p = 0.07$, $n = 4$) compared to saline ($n = 6$). Concordantly, the level of CD11c mRNA was markedly lower in the DM-0.1 versus saline treated group ($p < 0.05$). However, there were no differences between groups in the amount of Ly6g transcription, a marker of neutrophils (Fig. 3D). Treatment with DM-0.1 significantly reduced the levels of the T-lymphocyte markers CD4 (Fig. 3E) and CD8 mRNA (Fig. 3F), together with a downregulation of INF- γ (Fig. 3G) and IL17 (Fig. 3H) transcription. CCL2 is the chemokine secreted by astrocytes and a predominant driver of monocytes and lymphocytes into the CNS (Ransohoff et al., 1993). Treatment with DM-0.1 could prevent the upregulation of CCL2 mRNA in the spinal cord tissue of *EAE-II* mice (Fig. 3I). Hence, our data showed that the neuroprotective effect of DM-0.1 treatment was associated with an inhibition of cell trafficking into the CNS.

Low doses of DM inhibit NADPH oxidase mediated production of superoxide and the transcription of NOX2 subunits in microglia *in vitro* and in the spinal cord tissue

Next, we investigated whether the effect of low dose DM in *EAE-II* might involve the regulation of NOX2 activity. In the CNS of patients with MS and during EAE microglia are activated in response to INF- γ released by effector T-cells that in turn initiates inflammation and oxidative stress (Gonsette, 2008). Therefore, we first investigated whether DM can inhibit the NOX2 mediated release of superoxide in microglia *in vitro* after stimulation with INF- γ using a lucigenin-enhanced enzymatic assay. We observed a significant decrease in the production of superoxide by NOX2 when microglia were pretreated with DM before stimulation (Fig. 4A). In concentrations of $10^{-6} - 10^{-15}$ M, DM significantly inhibited the activity of NADPH oxidase ($p < 0.05$ versus INF- γ). This effect was comparable to the effect of antioxidant apocynin. DM at 10^{-9} and 10^{-10} M could dramatically inhibit p47phox mRNA (Fig. 4B; $p < 0.05$ versus INF- γ). At doses of $10^{-5} - 10^{-10}$ M, DM significantly downregulated the transcription of the NOX2 enzymatic subunit gp91phox (Fig. 4C; $p < 0.05$ for $10^{-5} - 10^{-8}$ M and $p < 0.01$ for 10^{-9} and 10^{-10} M). We also observed a decrease of iNOS transcription in DM treated microglia (Fig. 4D). Expression and activity of NOX2 was further investigated in the spinal cord tissue of EAE animals collected at the peak of disease. Treatment with DM-0.1 could significantly reduce the mRNA level of p47phox ($p < 0.05$; $n = 4$) in comparison to saline ($n = 6$) in the spinal cords of EAE animals (Fig. 5A). We also observed a decreased level of gp91phox mRNA after DM-0.1 treatment (Fig. 5B; $p = 0.07$). However, we could not observe a significant inhibition of NOX2 enzymatic activity and production of superoxide in the spinal cord tissue of DM-0.1 treated group compared to saline (Fig. 5C). Nevertheless, the level of iNOS mRNA was dramatically reduced after treatment with the low dose DM (Fig. 5D; $p < 0.05$). Thus we found that DM could inhibit NOX2-mediated production of superoxide and the transcription of NOX2 subunits in microglia *in vitro* after stimulation with INF- γ . Low doses of DM were the most effective. We also observed a reduction of p47phox and gp91phox mRNA together with an inhibition of oxidative stress by DM-0.1 in the spinal cord tissue of EAE animals after DM-0.1 treatment.

Chronic treatment with DM-0.1 attenuates axonal demyelination and reduces neutrophil CNS infiltration of animals with EAE of moderate severity

Spinal cords of mice treated with saline, DM-10 or DM-0.1 were examined for cell infiltration, demyelination and axonal loss at the end of the experiment (45 d. p. i.). Reduction of Iba1⁺ macrophages/microglia was revealed by immunohistochemistry in animals treated with DM-10 (Fig. 6B) or DM-0.1 (Fig. 6C) in contrast to saline (Fig. 6A). Round Iba1⁺ cells with macrophage morphology were observed in the subarachnoid space around spinal cord in all experimental groups. However, some large round Iba1⁺ cells were found in the spinal cord parenchyma of saline treated animals. Nevertheless, analysis of qPCR showed no differences in the expression of CD11b mRNA (Fig. 6D) between DM-10, DM-0.1 and Saline treated groups ($n = 4/\text{group}$). Chronic treatment with DM-10 or DM-0.1 did not change the amount of infiltrating immune cells expressing CD45 (Fig. 6E), but significantly reduced the amount of Ly6g expressing neutrophils in the spinal cord tissue when compared to saline (Fig. 6F; $p < 0.05$ for DM-10 and $p < 0.01$ for DM-0.1). Large areas of myelin loss and abnormal myelin were found in the ventrolateral lumbar spinal cords of saline treated animals at 45 d.p.i. (Fig. 6G). In comparison to saline, chronic treatment with DM-10 (Fig. 6H) or DM-0.1 (Fig. 6I) markedly decreased the level of demyelination in the spinal cords of *EAE-II* mice. However, only DM-0.1 treatment could prevent axonal loss that was seen in demyelinating areas of the spinal cords of both the saline and DM-10 groups (Fig. 6G, 6H, 6L) using the SMI-312 staining of highly phosphorylated axonal epitopes of neurofilaments (Ulfig et al., 1998). Upregulation in the transcription of sigma-1 receptors might imply that regenerative mechanisms and remyelination could have also occurred after chronic treatment with DM-0.1 (Fig. 6J).

Taking together, our data showed that low dose DM (DM-0.1) was neuroprotective in moderate EAE, which was associated with low infiltration of peripheral immune cells. Chronic treatment with DM-0.1 could inhibit NOX2 expression and the enzymatic activity in the spinal cord tissue, and thus resulted in a reduction of oxidative stress and the subsequent inhibition of infiltration in the CNS, preventing severe demyelination and axonal loss.

Discussion

Here we demonstrated the novel protective effects of the morphine derivative DM at a low dose against moderate EAE. We also showed that this effect of low dose DM was associated with an inhibition of NOX2, a decrease of CNS infiltration and a reduction of demyelination and axonal degeneration in the spinal cords of EAE mice. DM is clinically available and well tolerated, and has already demonstrated neuroprotective properties in various experimental models of neurological diseases. Our findings may provide exciting information leading to a new, inexpensive strategy for treating MS.

The unique ability of low dose morphinans to regulate inflammation through inhibition of the NOX2-dependent production of ROS could contribute importantly to the potential of these compounds to treat autoimmune diseases, such as MS. Apart from LDN, whose neuroprotective activity in MS and EAE has been suggested to involve the blockade of opioid receptors (Rahn et al., 2011; Zagon et al., 2009), little is known about the ability of other morphinans to treat MS. We investigated the effect of the dextrorotary morphinan and non-opioid cough suppressant DM on the development and progression of EAE. We induced EAE using C57BL/6 mice that are well known to be susceptible to MOG peptide-induced EAE and to develop disease phenotypes characterized by profound demyelination and axonal loss (Gold et al., 2006). We demonstrated that well-established doses of MOG (300 µg) and M.t. (2.5–5 mg/ml) resulted in the development of *EAE-I* that displayed a chronic-progressive pattern of clinical symptoms (Berard et al., 2010; Gold et al., 2006; Soulika et

al., 2009). During the chronic phase of *EAE-I*, we found large amounts of infiltrating neutrophils and CD4⁺, CD8⁺ T-lymphocytes in the spinal cord. Recent reports demonstrated that neutrophils are involved in the pathology of EAE that is mediated mostly by Th17 effector cells and their regulatory mediator IL17. This type of EAE would likely resemble progressive form of MS (Jager et al., 2009; Jager and Kuchroo, 2010). The lack of a therapeutic effect of DM in *EAE-I* leads to the conclusion that treatment with DM might not be sufficient enough to inhibit inflammation in the presence of high numbers of infiltrating immune cells including neutrophils. Minor attenuation of clinical symptoms at the later time point when some infiltrating cells clear the CNS parenchyma might be in support of this hypothesis (Soulika et al., 2009). A certain level of microglial activation could change the ability of microglia to respond properly to DM treatment. In addition, ROS can also be involved in the regulation of anti-inflammatory mechanisms. It has been shown that ROS produced by macrophages might control the activity and apoptosis of encephalitogenic T-lymphocytes (Gelderman et al., 2007). Therefore, elimination of ROS might result in an exacerbation of disease symptoms, which has been shown in mice carrying a mutation in p47phox encoding gene Ncf1 (Hultqvist et al., 2004).

In *EAE-II*, reduced amounts of MOG (50 µg) and M.t. (0.5 mg/ml) led to alleviated severity and decreased incidence of the developed disease and resulted in moderate EAE in mice. *EAE-II* was characterized by lower numbers of T-lymphocytes, less activation of microglia and no significant amount of neutrophils in the spinal cord. It was suggested that this EAE, characterized by low neutrophil infiltration in the CNS, would possibly be mediated by Th1 cells and regulated mainly by IFN-γ (Jager and Kuchroo, 2010), although we observed an upregulation of IL17 under *EAE-II* conditions as well. This type of EAE could to some extent resemble the pathology of RRMS (Jager and Kuchroo, 2010). We found that the moderate pathology of *EAE-II* was suitable to reveal the beneficial effect of DM-0.1. Being administered i.p. starting from day 7 after immunization, DM-0.1 could prevent the development of the peak and slightly attenuate the progression of *EAE-II* clinical symptoms. At 7 d.p.i., MOG specific auto-reactive Th1, Th17 and Th1/Th17 lymphocytes are already present in the spleen and lymph nodes of EAE mice and can be detected in the brain and spinal cord at 10–14 d.p.i. (Murphy et al., 2010; Soulika et al., 2009). Therefore, we examined whether DM-0.1 treatment might target the transmigration of leukocytes into the CNS rather than the antigen presentation. Indeed, we found that there was a substantial decrease of CNS infiltration including macrophages, dendritic cells, CD4⁺ and CD8⁺ T-lymphocytes observed at the peak of EAE after DM-0.1 treatment. Moreover, downregulation of CCL2 expression found in the spinal cord tissue at this time point indicated that DM-0.1 treatment would likely regulate pro-inflammatory chemokines that drive the recruitment of inflammatory cells into the CNS. Since the onset of myelin and axonal loss take place immediately after CNS infiltration of peripheral immune cells, prevention of initial leukocytes transmigration by DM-0.1 in our study resulted in decrease of demyelination, attenuation of axonal degeneration and alleviation of EAE clinical symptoms.

Remarkably, the amount of neutrophils observed in the spinal cords during the chronic phase of *EAE-II* was higher compared to the numbers of neutrophils found at the peak of disease. It has been shown that neutrophils accumulating in the CNS during EAE contribute to exacerbation of neuronal loss and inhibit remyelination after injury (Liu et al., 2010). Interestingly, chronic treatment with DM-0.1 was effective to reduce the amount of neutrophils present in the spinal cord of *EAE-II* mice. Even though no differences in the clinical scores between the saline and DM-0.1-treated group were seen at the terminal time point of *EAE-II*, we found less demyelinating plaques and less accumulation of IBA1⁺ microglia/macrophages at the site of demyelination in the spinal cords after treatment with DM. Chronic DM-0.1 treatment could also regulate regenerative mechanisms in the spinal

cord tissue during EAE. Increased levels of sigma-1 receptor mRNA have been shown to be involved in the maturation of oligodendrocytes and cell survival (Hayashi and Su, 2004; Hayashi and Su, 2007).

The ability of DM to block NMDA receptors and inhibit voltage gated Ca-channels would unlikely be responsible for the protective effect of DM-0.1, because the low dose of compound was used and because high dose DM treatment did not show similar effect. Our data support the hypothesis that inhibition of NADPH oxidase might be an important mechanism involved in the neuroprotective effect of low dose DM in MS. The ability of low doses of morphine derivatives to inhibit the production of NOX2 derived ROS in cultured microglia and macrophages activated by LPS has been shown (Li et al., 2005; Liu et al., 2009). We demonstrated that DM in low doses from 10^{-6} M to 10^{-15} M can inhibit the NOX2 mediated production of superoxide in microglia activated by INF- γ . In addition, we showed that a 24-h treatment with low doses of DM could reduce the transcription level of NOX2 subunits and decrease iNOS gene expression, consistent with the previous observation that superoxide was involved in the regulation of NO production (Pawate et al., 2004). We demonstrated that the beneficial effect of DM-0.1 treatment in EAE was associated with a reduction of the transcription level of p47phox and gp91phox subunits of NADPH oxidase at the peak of the disease. We also showed an inhibition of the production of NOX2-dependent superoxide in the spinal cord tissue of DM-0.1 treated animals and a reduction of the iNOS transcription level, indicating the attenuation of inflammation and oxidative stress. Although our data have demonstrated the effect of low dose DM in microglia *in vitro*, we cannot exclude the possibility that DM-0.1 treatment could also target the expression and activity of NOX2 NADPH oxidase present on other immune cells, including macrophages, neutrophils or B-lymphocytes.

The fact that high dose DM failed to provide protection against both of the severe and the moderate EAEs suggests that unwanted effects of the compound might have been more obvious when high dose DM was used, and also indicates that DM treatment might unlikely work through the antagonism of NMDA receptors.

Overall, our results reveal a novel protective effect of low dose DM in autoimmune CNS inflammation, and demonstrate that a possible mechanism of action is via inhibition of NADPH oxidase and decrease of CNS leukocytes infiltration. These exciting findings may provide useful information leading to a new, inexpensive strategy for treating MS.

Acknowledgments

The authors thank Dr. Vimal Selvaraj and Dr. Athena Soulika for insightful suggestions, Joy X. Jiang for help in establishing lucigenin-enhanced chemiluminescence assay, John Avery for technical assistance and Eunyoung Lee for providing the CCL2 primers and CD4 antibody. This work was in part supported by grants to W.D. from the National Institutes of Health (R01NS061983, R01ES015988), National Multiple Sclerosis Society, and Shriners Hospitals for Children.

Abbreviations

DM	dextromethorphan
DM-10	dextromethorphan, i.p. at 10 mg/kg
DM-0.1	dextromethorphan, i.p. at 0.1 mg/kg
d.p.i	days post immunization
EAE	experimental autoimmune encephalomyelitis

LDN	low dose naltrexone
LFB	luxol fast blue
MBP	myelin basic protein
MS	multiple sclerosis
ROS	reactive oxygen species

References

- Bedard K, Krause KH. The NOX family of ROS-generating NADPH oxidases: physiology and pathophysiology. *Physiol Rev.* 2007; 87:245–313. [PubMed: 17237347]
- Benveniste EN. Role of macrophages/microglia in multiple sclerosis and experimental allergic encephalomyelitis. *J Mol Med.* 1997; 75:165–73. [PubMed: 9106073]
- Berard JL, et al. Characterization of relapsing-remitting and chronic forms of experimental autoimmune encephalomyelitis in C57BL/6 mice. *Glia.* 2010; 58:434–45. [PubMed: 19780195]
- Britton P, et al. Dextromethorphan protects against cerebral injury following transient, but not permanent, focal ischemia in rats. *Life Sci.* 1997; 60:1729–40. [PubMed: 9150412]
- Gandhi R, et al. Role of the innate immune system in the pathogenesis of multiple sclerosis. *J Neuroimmunol.* 2010; 221:7–14. [PubMed: 19931190]
- Gelderman KA, et al. Macrophages suppress T cell responses and arthritis development in mice by producing reactive oxygen species. *J Clin Invest.* 2007; 117:3020–8. [PubMed: 17909630]
- Gold R, et al. Understanding pathogenesis and therapy of multiple sclerosis via animal models: 70 years of merits and culprits in experimental autoimmune encephalomyelitis research. *Brain.* 2006; 129:1953–71. [PubMed: 16632554]
- Gonsette RE. Neurodegeneration in multiple sclerosis: the role of oxidative stress and excitotoxicity. *J Neurol Sci.* 2008; 274:48–53. [PubMed: 18684473]
- Hattori H, et al. Reactive oxygen species as signaling molecules in neutrophil chemotaxis. *Commun Integr Biol.* 2010; 3:278–81. [PubMed: 20714413]
- Hayashi T, Su TP. Sigma-1 receptors at galactosylceramide-enriched lipid microdomains regulate oligodendrocyte differentiation. *Proc Natl Acad Sci U S A.* 2004; 101:14949–54. [PubMed: 15466698]
- Hayashi T, Su TP. Sigma-1 receptor chaperones at the ER-mitochondrion interface regulate Ca(2+) signaling and cell survival. *Cell.* 2007; 131:596–610. [PubMed: 17981125]
- Hultqvist M, et al. Enhanced autoimmunity, arthritis, and encephalomyelitis in mice with a reduced oxidative burst due to a mutation in the *Ncf1* gene. *Proc Natl Acad Sci U S A.* 2004; 101:12646–51. [PubMed: 15310853]
- Huppert J, et al. Cellular mechanisms of IL-17-induced blood-brain barrier disruption. *FASEB J.* 2010; 24:1023–34. [PubMed: 19940258]
- Jager A, et al. Th1, Th17, and Th9 effector cells induce experimental autoimmune encephalomyelitis with different pathological phenotypes. *J Immunol.* 2009; 183:7169–77. [PubMed: 19890056]
- Jager A, Kuchroo VK. Effector and regulatory T-cell subsets in autoimmunity and tissue inflammation. *Scand J Immunol.* 2010; 72:173–84. [PubMed: 20696013]
- Kim HC, et al. Metabolism to dextromethorphan is not essential for dextromethorphan's anticonvulsant activity against kainate in mice. *Life Sci.* 2003; 72:769–83. [PubMed: 12479976]
- Kim HC, et al. The effects of dextromethorphan on kainic acid-induced seizures in the rat. *Neurotoxicology.* 1996; 17:375–85. [PubMed: 8856734]
- Lam GY, et al. The many roles of NOX2 NADPH oxidase-derived ROS in immunity. *Semin Immunopathol.* 2010; 32:415–30. [PubMed: 20803017]
- Li G, et al. Femtomolar concentrations of dextromethorphan protect mesencephalic dopaminergic neurons from inflammatory damage. *Faseb J.* 2005; 19:489–96. [PubMed: 15790998]

- Liu B, et al. Naloxone protects rat dopaminergic neurons against inflammatory damage through inhibition of microglia activation and superoxide generation. *J Pharmacol Exp Ther.* 2000; 293:607–17. [PubMed: 10773035]
- Liu B, Hong JS. Neuroprotective effect of naloxone in inflammation-mediated dopaminergic neurodegeneration. Dissociation from the involvement of opioid receptors. *Methods Mol Med.* 2003; 79:43–54. [PubMed: 12506689]
- Liu L, et al. CXCR2-positive neutrophils are essential for cuprizone-induced demyelination: relevance to multiple sclerosis. *Nat Neurosci.* 2010; 13:319–26. [PubMed: 20154684]
- Liu SL, et al. Dextromethorphan reduces oxidative stress and inhibits atherosclerosis and neointima formation in mice. *Cardiovasc Res.* 2009; 82:161–9. [PubMed: 19189960]
- Liu Y, et al. Dextromethorphan protects dopaminergic neurons against inflammation-mediated degeneration through inhibition of microglial activation. *J Pharmacol Exp Ther.* 2003; 305:212–8. [PubMed: 12649371]
- Livak KJ, Schmittgen TD. Analysis of relative gene expression data using real-time quantitative PCR and the 2(-Delta Delta C(T)) Method. *Methods.* 2001; 25:402–8. [PubMed: 11846609]
- Mirshafiey A, Mohsenzadegan M. Antioxidant therapy in multiple sclerosis. *Immunopharmacol Immunotoxicol.* 2009; 31:13–29. [PubMed: 18763202]
- Murphy AC, et al. Infiltration of Th1 and Th17 cells and activation of microglia in the CNS during the course of experimental autoimmune encephalomyelitis. *Brain Behav Immun.* 2010; 24:641–51. [PubMed: 20138983]
- Narita M, et al. Up-regulation of spinal mu-opioid receptor function to activate G-protein by chronic naloxone treatment. *Brain Res.* 2001; 913:170–3. [PubMed: 11549382]
- Pawate S, et al. Redox regulation of glial inflammatory response to lipopolysaccharide and interferongamma. *J Neurosci Res.* 2004; 77:540–51. [PubMed: 15264224]
- Qian L, et al. Microglia-mediated neurotoxicity is inhibited by morphine through an opioid receptor-independent reduction of NADPH oxidase activity. *J Immunol.* 2007; 179:1198–209. [PubMed: 17617613]
- Qin L, et al. Microglial NADPH oxidase is a novel target for femtomolar neuroprotection against oxidative stress. *Faseb J.* 2005; 19:550–7. [PubMed: 15791005]
- Rahn KA, et al. Prevention and diminished expression of experimental autoimmune encephalomyelitis by low dose naltrexone (LDN) or opioid growth factor (OGF) for an extended period: Therapeutic implications for multiple sclerosis. *Brain Res.* 2011
- Rajashekara V, et al. Chronic opioid antagonist treatment dose-dependently regulates mu-opioid receptors and trafficking proteins in vivo. *Pharmacol Biochem Behav.* 2003; 75:909–13. [PubMed: 12957235]
- Ransohoff RM, et al. Astrocyte expression of mRNA encoding cytokines IP-10 and JE/MCP-1 in experimental autoimmune encephalomyelitis. *FASEB J.* 1993; 7:592–600. [PubMed: 8472896]
- Savina A, et al. NOX2 controls phagosomal pH to regulate antigen processing during cross presentation by dendritic cells. *Cell.* 2006; 126:205–18. [PubMed: 16839887]
- Selvaraj V, et al. PARP-1 deficiency increases the severity of disease in a mouse model of multiple sclerosis. *J Biol Chem.* 2009; 284:26070–84. [PubMed: 19628872]
- Souluka AM, et al. Initiation and progression of axonopathy in experimental autoimmune encephalomyelitis. *J Neurosci.* 2009; 29:14965–79. [PubMed: 19940192]
- Steinberg GK, et al. Dextromethorphan protects against cerebral injury following transient focal ischemia in rabbits. *Stroke.* 1988; 19:1112–8. [PubMed: 3413809]
- Szczucinski A, Losy J. Chemokines and chemokine receptors in multiple sclerosis. Potential targets for new therapies. *Acta Neurol Scand.* 2007; 115:137–46. [PubMed: 17295707]
- Topsakal C, et al. Effects of methylprednisolone and dextromethorphan on lipid peroxidation in an experimental model of spinal cord injury. *Neurosurg Rev.* 2002; 25:258–66. [PubMed: 12172735]
- Ulfig N, et al. Monoclonal antibodies SMI 311 and SMI 312 as tools to investigate the maturation of nerve cells and axonal patterns in human fetal brain. *Cell Tissue Res.* 1998; 291:433–43. [PubMed: 9477300]

- van der Veen RC, et al. Superoxide prevents nitric oxide-mediated suppression of helper T lymphocytes: decreased autoimmune encephalomyelitis in nicotinamide adenine dinucleotide phosphate oxidase knockout mice. *J Immunol.* 2000; 164:5177–83. [PubMed: 10799876]
- Werling LL, et al. Dextromethorphan as a potential neuroprotective agent with unique mechanisms of action. *Neurologist.* 2007; 13:272–93. [PubMed: 17848867]
- Zagon IS, et al. Endogenous opioids regulate expression of experimental autoimmune encephalomyelitis: a new paradigm for the treatment of multiple sclerosis. *Exp Biol Med* (Maywood). 2009; 234:1383–92. [PubMed: 19855075]
- Zhang W, et al. Neuroprotective effect of dextromethorphan in the MPTP Parkinson's disease model: role of NADPH oxidase. *Faseb J.* 2004; 18:589–91. [PubMed: 14734632]

Research Highlights

- Low dose dextromethorphan attenuates autoimmune CNS inflammation
- Inhibits expression and activity of NOX2
- Suppresses infiltration of peripheral immune cells into the CNS
- Reduces demyelination and axonal loss
- May be a new, inexpensive strategy for treating multiple sclerosis

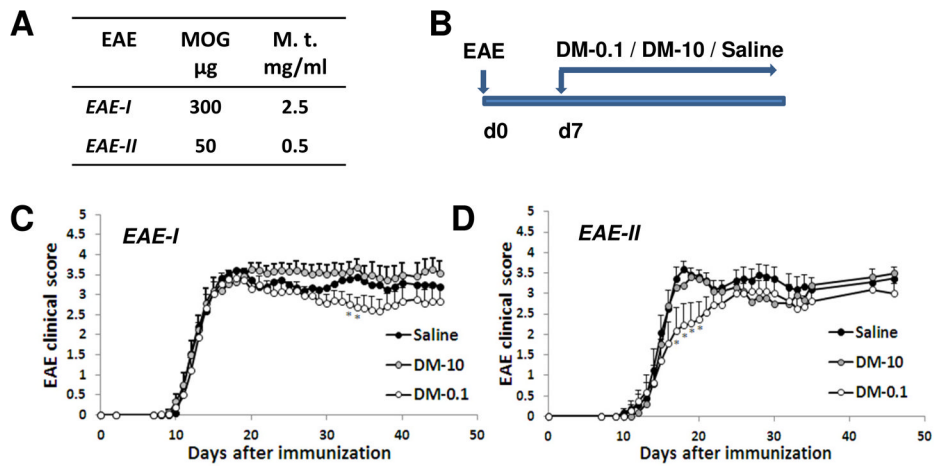


Figure 1. Effect of DM-10 or DM-0.1 treatment on the development and progression of EAE
 The therapeutic effect of DM was investigated in two types of EAE, which were induced by using different concentrations of MOG peptide and M.t. (A). Animals received a daily i.p. injection of a high dose 10 mg/kg (DM-10) or a low dose 0.1 mg/kg (DM-0.1) of DM or saline beginning from 7 d.p.i. until the end of the experiment (45 days) (B). DM-0.1 treatment showed a minor late attenuation clinical symptoms of *EAE-I*, a chronic-progressive form of severe EAE ($n=22$ /group) (C). DM-10 was not effective in this form of EAE. In a less severe form, in *EAE-II*, treatment with DM-0.1 showed a moderate early attenuation of the disease clinical symptoms that was the most prominent at the peak ($n=22-23$ /group) (D). Treatment with DM-10 did not affect the *EAE-II* clinical score, although some amelioration of the symptoms could be seen temporally after the peak of disease. *, $p < 0.05$ versus the same time point in the saline treated group.

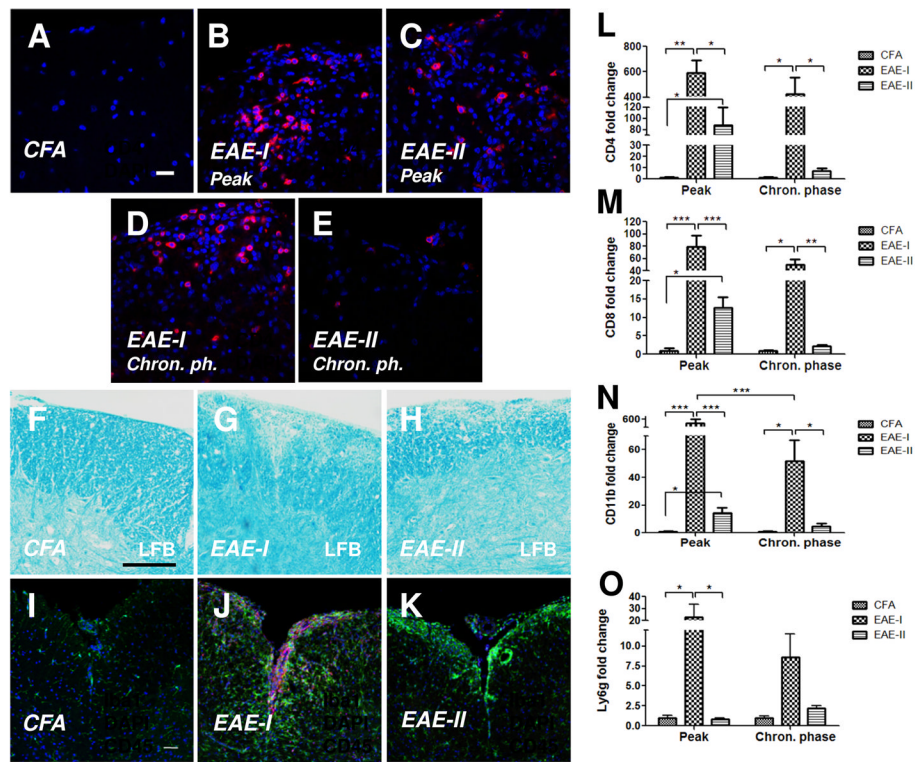


Figure 2. EAE-I is characterized by severe demyelination and massive spinal cord infiltration
Lumbar spinal cords of saline treated mice in the CFA control, *EAE-I* and *EAE-II* groups were examined for demyelination and mononuclear cell infiltration at the peak and the chronic phase of EAE (day 45). CD4⁺ T-cells were found in the spinal cord parenchyma of *EAE-I* (B, D) and *EAE-II* (C, E) animals at both time points. No CD4 expressing cells were observed in the CFA-control (A). Demyelinating plaques were detected in the spinal cords during the chronic phase of EAE using LFB staining (F-H). Higher level of myelin loss was found in *EAE-I* (G) compared to *EAE-II* (H). In addition, a dramatic increase of Iba⁺ macrophages/microglia was shown throughout the coronal sections of the spinal cords in *EAE-I* (J) vs *EAE-II* (K). The number of CD45⁺ cells (I-K) was also markedly elevated in *EAE-I* spinal cords when compared to the CFA control or *EAE-II*. qPCR analysis revealed increased levels of mRNAs encoding CD4 (L), CD8 (M), CD11b (N) proteins in *EAE-I* and *EAE-II* animals at the peak of disease ($n = 4-7$). Cell infiltration in *EAE-I* was significantly higher when compared to *EAE-II*. An increase of Ly6g mRNA level was detected only in *EAE-I* animals at the peak of disease (O). *, $p < 0.05$; **, $p < 0.01$ and ***, $p < 0.001$. Scale bars: A-E, D-L, 50 μm ; F-H, 200 μm .

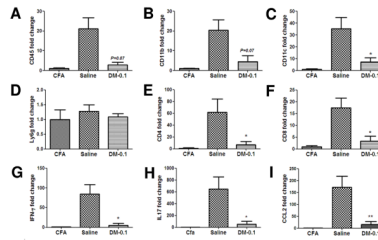


Figure 3. Neuroprotective effect of DM-0.1 in EAE-II is associated with the inhibition of cellular infiltration into the CNS

EAE was induced by a low dose of MOG and M.t. (*EAE-II*, Fig. 1A). Cell infiltration in the spinal cords of mice treated with DM-0.1 or saline was examined at the peak of EAE (19–20 d.p.i.). Levels of mRNAs encoding proteins specific for different cell populations were detected by qPCR. A dramatic decrease of CD45 (A), CD11b (B) and CD11c (C) gene transcription was revealed after DM-0.1 treatment ($n = 4$). However, DM-0.1 did not change the expression of the neutrophil specific Ly6g gene (D) when compared to Saline ($n = 6$). Significant decrease of CD4 (E) and CD8 (F) expressing T-lymphocytes was observed together with a reduction of transcription of IFN- γ (G) and IL17 (H) after DM-0.1 treatment. Decrease of cellular infiltration into CNS was associated with a reduction of expression of CCL2 mRNA in the spinal cord tissue (I). *, $p < 0.05$ and **, $p < 0.01$ versus the saline group.

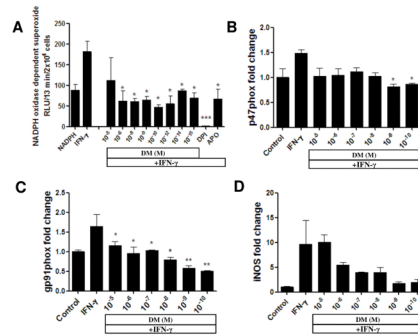


Figure 4. DM inhibits the transcription of NOX2 subunits and NOX2-mediated production of superoxide in microglia *in vitro*

Superoxide production in microglia was measured using lucigenin-enhanced chemiluminescence assay. DM at the concentrations from 10⁻⁶ to 10⁻¹⁵ M could significantly downregulate NOX2 mediated superoxide production, when microglia were treated with DM for 2 h before stimulation with 20 ng/ml IFN-γ (A). Primary microglia were pre-incubated for 2 h with different concentrations of DM before further treatment with 20 ng/ml IFN-γ for the next 22 h. Total RNA was isolated and expression of the genes encoding NADPH oxidase subunits p47phox and gp91phox was analyzed by qPCR. DM at the concentration of 10⁻⁹ or 10⁻¹⁰ M significantly inhibited the transcription of p47phox subunit (B). The transcription level of gp91phox was significantly downregulated by a wide range of DM concentrations from 10⁻⁵ to 10⁻¹⁰ M (C). DM treatment also resulted in a reduction of iNOS mRNA (D). *, $p < 0.05$; **, $p < 0.01$ versus the IFN-γ treated group.

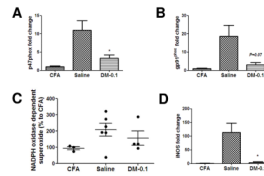


Figure 5. DM-0.1 inhibits the expression of NOX2 and oxidative stress response in the spinal cord tissue of EAE-II animals

Mice were immunized with 50 μ g MOG/0.5 mg/ml M.t. and treated with saline or DM-0.1 starting from day 7 until the peak of EAE (19–20 d.p.i.). Lumbar spinal cords were collected after perfusion with PBS and analyzed for the expression and activity of NOX2. DM-0.1 treatment ($n = 4$) could significantly reduce the mRNA level of p47phox in the spinal cord tissue when compared to saline ($n = 6$) (A). The transcription level of the enzymatic subunit gp91phox was also decreased in the spinal cord tissue after DM-0.1 treatment (B). A non-significant reduction in NADPH oxidase-dependent superoxide production was found in the spinal cord homogenates of DM-0.1 treated animals (D). The transcription level of iNOS was dramatically decreased by DM-0.1 treatment (E). *, $p < 0.05$ versus the saline group.

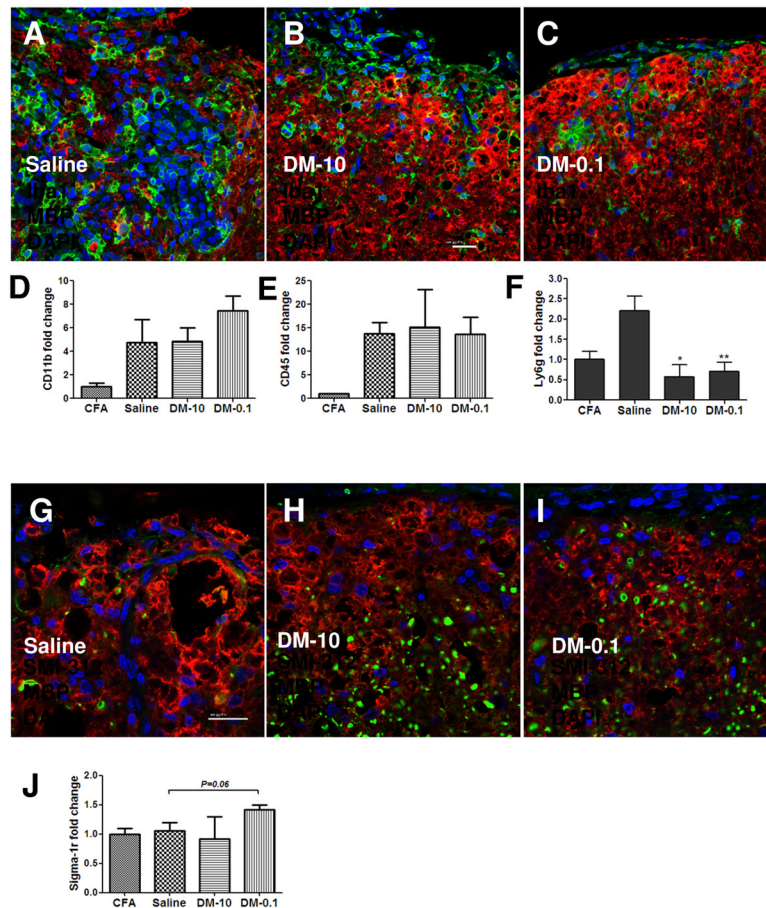


Figure 6. Chronic DM-0.1 treatment reduces neutrophil infiltration and axonal degeneration, and stimulates regeneration in the spinal cords of animals with EAE of moderate severity Lumbar spinal cords of *EAE-II* mice treated with saline, DM-10 or DM-0.1 were analyzed for cell infiltration and demyelination at the end of the experiment (45 d.p.i.). Accumulation of Iba1⁺ cells in the subarachnoid space was found in the spinal cords of all experimental groups (A-C). A lot of large round Iba1⁺ cells with macrophage morphology were observed in the site of demyelination in the spinal cords of Saline treated animals (A). However, no significant differences in the amount of macrophages/microglia between saline and DM-treated groups were revealed by q-PCR (D). Although no differences in the CD45 gene expression level (E) were observed between groups, there was noted reduction in the amount of Ly6g mRNA (F) expressed by infiltrating neutrophils ($n = 4/\text{group}$; *, $p < 0.05$ and **, $p < 0.01$ versus the saline group). Less demyelination was revealed by MBP immunohistochemistry in DM-10 and DM-0.1 treated animals compared to the saline group (G-I). A higher fraction of myelinated MBP-SMI-312⁺ axons was found in ventrolateral spinal cords of animals treated with DM-0.1 (I) in comparison to saline (G) or DM-10 (H). Upregulation of sigma-1 receptor (sigma-1r) mRNA level was detected in the spinal cords of DM-0.1 treated animals (J). Scale bars: A-C and G-I, 20 μm .

Table 1

Clinical characteristics of EAE-I

<i>EAE-I</i>	n	Incidence %	Mean number of days to onset	Mean score at the peak of disease	Mean maximal severity score	Duration of paralysis	Mean score at the end of experiment	Survival %
Saline	22	100	12.4 ± 0.4	3.6 ± 0.1	4.2 ± 0.1	12.5 ± 1.6	3.2 ± 0.2	82
DM-10	22	100	13.0 ± 0.6	3.3 ± 0.3	4.2 ± 0.1	14.3 ± 1.9	3.5 ± 0.3	68
DM-0.1	22	100	13.1 ± 0.6	3.4 ± 0.2	4.0 ± 0.2	10.4 ± 1.8	2.8 ± 0.3	86
<i>P-value</i>			NS	NS	NS	NS	NS	NS

Data represent the mean ± SEM. NS – not significant.

Table 2

Clinical characteristics of EAE-II

EAE-II	n	Incidence %	Mean number of days to onset	Mean score at the peak of disease	Mean maximal severity score	Duration of paralysis	Mean score at the end of experiment	Survival %
Saline	23	96	14.6 ± 0.6	3.6 ± 0.2	4.1 ± 0.1	9.9 ± 2.1	3.4 ± 0.3	91
DM-10	22	100	15.0 ± 0.6	3.2 ± 0.4	4.1 ± 0.1	9.2 ± 1.6	3.5 ± 0.2	100
DM-0.1	22	96	16.6 ± 1.3	2.2 ± 0.5*	3.7 ± 0.2	7.7 ± 1.6	3.0 ± 0.3	96
<i>P-value</i>			NS	< 0.05	NS	NS	NS	NS

Data represent the mean ± SEM.

* significant difference compared to the saline group ($p < 0.05$); NS – not significant.